

Classification of Tear Film Lipid Layer En Face Maps Obtained Using Optical Coherence Tomography and Their Correlation With Clinical Parameters

Hannes Stegmann,*† Valentin Aranha Dos Santos,*† Doreen Schmidl,‡ Gerhard Garhöfer,‡ Ali Fard,§ Homayoun Bagherinia,§ Leopold Schmetterer,*†¶||**††‡‡ and René M. Werkmeister*†

Purpose: The purpose of this study was to investigate the correlation between the pattern of optical coherence tomography (OCT) en face maps of the tear film lipid layer (TFLL) and lipid layer thickness (LLT), fluorescein breakup time (FBUT), and Schirmer I test values in healthy subjects.

Methods: Measurements from four clinical data sets were retrospectively analyzed, and TFLL patterns were classified into 3 categories: homogeneous (HOM), wavy (WAV), or dotted (DOT) appearance. Linear mixed model analyses were performed. Intraclass correlation coefficients and index of qualitative variation were computed to investigate interrater and intrasubject variabilities.

Results: For the LLT, a significant difference between HOM and DOT ($P < 0.001$, $\beta_{\text{HOMvsDOT}} = -6.42$ nm) and WAV and DOT

($P = 0.002$, $\beta_{\text{WAVvsDOT}} = -4.04$ nm) was found. Furthermore, the difference between WAV and DOT regarding FBUT ($P < 0.001$, $\beta_{\text{WAVvsDOT}} = -3.065$ seconds) was significant, while no significant differences between any of the classes with respect to the Schirmer I test values were found. An intraclass correlation coefficient of 89.0% reveals a good interrater reliability, and an index of qualitative variation of 60.0% shows, on average, a considerable variability in TFLL pattern class for repeated measurements over 1 hour.

Conclusions: A new classification method for OCT en face maps of the TFLL is presented. Significant differences between patterns were found with respect to LLT and FBUT. A dotted pattern on dark background appears to be the most stable type of TFLL. The analysis of OCT en face maps of the TFLL provides complimentary information to conventional imaging methods and might give new insights into the characteristics of the TFLL.

Key Words: tear film, tear film lipid layer, lipid layer pattern, lipid layer thickness, optical coherence tomography, reflectance

(*Cornea* 2023;42:490–497)

INTRODUCTION

The precorneal tear film is an essential part of the ocular surface. It not only provides a smooth boundary at the air–tear interface, which is crucial for the optics of the eye,¹ but also prevents the cornea from desiccating, protects against bacterial infections,² and has a nutritional role.³ Four layers constitute the tear film: the glycocalyx, the mucous layer, the aqueous layer, and the lipid layer.⁴ The latter, as its outermost layer, is an essential element of the tear film and has a thickness typically ranging from 15 to 157 nm.⁵ It is responsible for the stabilization of the tear film by lowering the surface tension of the tear fluid and creates a smooth surface at the air–tear interface. It is believed to help slow the evaporation of the aqueous layer,⁶ although this is not without controversy and could not be reproduced *in vitro*.⁷ Not only its thickness but also the composition of lipids seems to play a key role for the characteristics of the lipid layer.^{5,8}

The major part of the tear film lipid layer (TFLL) consists of the meibomian secretion, often called meibum, which originates from the meibomian glands in the upper and lower eyelids and comprises nonpolar and polar lipids as well as proteins.^{9–12} The origin of the non-meibomian lipids that are found in tears is still largely unknown.^{3,13} The meibomian

Received for publication July 13, 2022; revision received August 25, 2022; accepted August 31, 2022. Published online ahead of print November 21, 2022.

From the *Center for Medical Physics and Biomedical Engineering, Medical University of Vienna, Austria; †Christian Doppler Laboratory for Ocular and Dermal Effects of Thiomers, Medical University of Vienna, Austria; ‡Department of Clinical Pharmacology, Medical University of Vienna, Austria; §Carl Zeiss Meditec Inc, Dublin, CA; ¶Singapore Eye Research Institute, Singapore National Eye Centre, Singapore, Singapore; ||Nanyang Technological University, Singapore, Singapore; **Ophthalmology and Visual Sciences Academic Clinical Program, Duke-NUS Medical School, Singapore; ††SERI-NTU Advanced Ocular Engineering (STANCE), Singapore; and ‡‡Institute of Molecular and Clinical Ophthalmology, Basel, Switzerland.

The research was funded by the Christian Doppler Research Association, the Austrian Federal Ministry for Digital and Economic Affairs, and the National Foundation for Research and Technology and Development with Grant number CD10260502; Christian Doppler Laboratory for Ocular and Dermal Effects of Thiomers.

Conflicts of interest statement: The authors have no funding or conflicts of interest to disclose.

Supplemental digital content is available for this article. Direct URL citations appear in the printed text and are provided in the HTML and PDF versions of this article on the journal's Web site (www.corneajml.com).

The data sets generated and analyzed during this study are available from the corresponding author on reasonable request.

Correspondence: René M. Werkmeister, Center for Medical Physics and Biomedical Engineering, Medical University of Vienna, Währinger Gürtel 18-20, 1090 Vienna, Austria (e-mail: rene.werkmeister@meduniwien.ac.at).

Copyright © 2022 The Author(s). Published by Wolters Kluwer Health, Inc. This is an open access article distributed under the terms of the Creative Commons Attribution-Non Commercial-No Derivatives License 4.0 (CCBY-NC-ND), where it is permissible to download and share the work provided it is properly cited. The work cannot be changed in any way or used commercially without permission from the journal.

glands secrete the meibum onto the posterior lid margins and into the marginal tear reservoirs, from where it is spread through surface tension onto the tear film during the upward motion of a blink.⁶ The miscibility of the hydrophilic aqueous tears and the hydrophobic meibum is limited, which leads to the creation of a distinct lipid layer on top of the tear film, probably in the form of a complex and multilayered structure.¹⁰ It is still poorly understood how factors such as its composition and the temperature influence the formation and thickness of the TFLL.¹³ A quantitative or qualitative alteration of the meibum, and therefore of the TFLL, is one of the main causes of dry eye disease (DED), with studies indicating that anywhere from half to up to 86% of all DED cases show signs of meibomian gland dysfunction (MGD).^{14,15}

The very thin nature of the TFLL makes it challenging to image and to quantify it *in vivo*. Nonetheless, several methods have been developed over the years, for example, based on relative reflectance values⁵ or based on white light interferometry, such as the Tearscope Plus,¹⁶ Kowa DR-1,¹⁷ IDRA Ocular surface analyzer, or LipiView II system.¹⁸ The lipid pattern, i.e. the qualitative optical appearance of the TFLL, has also been used to differentiate between healthy subjects and patients with MGD. On the one hand, correlations between the lipid pattern and DED¹⁹ and, on the other hand, clear changes in the lipid pattern structure in the case of MGD²⁰ were reported. Several different classification methods of these TFLL patterns have been proposed. A nonexhaustive overview is presented in Table 1 for static images, while dynamic classification methods have also been proposed.^{21–23}

Optical coherence tomography (OCT) is a noninvasive imaging technology that has revolutionized ophthalmic imaging in the past 3 decades. It acquires volumetric data and can reach tissue resolutions in the micrometer range. When projecting the acquired volumetric data along the axial direction, so-called en face maps²⁴ can be created and used to visualize the *in vivo* TFLL.²⁵

In this article, we present a new classification model for TFLL en face maps acquired with OCT and investigate their correlation with clinical parameters such as TFLL thickness (LLT), fluorescein breakup time (FBUT), and Schirmer I test. To the best of our knowledge, this is the first time that a classification method based on OCT en face maps of the TFLL is proposed.

MATERIAL AND METHODS

Data set

We retrospectively analyzed 318 measurements from 54 healthy subjects (30 male, 24 female, age 31 ± 8 years). Measurements were acquired within the framework of three different study protocols. The studies were approved by the local ethics board and the competent authorities and were performed in adherence to the Declaration of Helsinki²⁸ and to the Good Clinical Practice guidelines. Study participants gave their written informed consent after explanation of the study rationale. Inclusion criteria for the healthy study participants were as follows: age at least 18 years, normal findings in the medical history, ametropia ≤6 dpt, and no

application of any eye drops or ointments in the 24 hours preceding the screening visit and the study day. Exclusion criteria were participation in a clinical trial in the 3 weeks preceding this study, symptoms of a clinically relevant illness in the 3 weeks before the first study day, wearing of contact lenses, intake of dietary supplements in the 3 months preceding this study, treatment with corticosteroids in the 4 weeks preceding this study, topical treatment with any ophthalmic drug in the 4 weeks preceding this study, ocular infection or clinically significant inflammation, ocular surgery in the 3 months preceding this study, DED, Sjögren syndrome, pregnancy, or planned pregnancy. Study measurements were performed in the following order so that one did not affect the other: ultrahigh-resolution OCT (UHR-OCT) imaging of the corneal surface, measurement of LLT using a LipiView II Ocular Surface Interferometer, measurement of FBUT, and Schirmer I test. OCT data were acquired with a custom-built UHR-OCT system described in detail elsewhere.^{29,30} The system provides axial and lateral tissue resolutions of 1.2 μm and 21 μm, respectively, and thus allows resolving the precorneal tear film, i.e. revealing clearly distinguishable signals for the front surface of the tear film and the front surface of the corneal epithelium. The reflectance of the TFLL overlying the aqueous layer is dependent on the refractive indices of the media air, lipid layer and aqueous layer, and the thickness of the lipid layer.²⁵ To generate the TFLL en face map, the air–tear interface of

TABLE 1. TFLL Pattern Classification in the Literature

Publication	Area	Number of Classes	Description of Classes
Yokoi et al, 1996 ¹⁹	2-mm diameter	5	1: Somewhat gray color, uniform distribution 2: Somewhat gray color, nonuniform distribution 3: A few colors, nonuniform distribution 4: Many colors, nonuniform distribution 5: Corneal surface partially exposed
Guillon, 1998 ¹⁶	Whole cornea	5 (7)	Open meshwork, closed meshwork, wave, amorphous, normal colors (globular, abnormal colors)
Thai et al, 2004 ²⁶	5.5-mm diameter	5	1: Islands on light background 2: Clusters of lipid on light wavy background 3: Micelles on wavy background 4: Even appearance with vague fringes 5: Evenly spread lipid layer, hardly any fringes
Remeseiro et al, 2014 ²⁷	5-mm diameter	5	Strong fringes, coalescing strong fringes, fine fringes, debris

the acquired corneal measurement is first detected in each cross-sectional image of the volume and then fitted to a parabolic shape to correct potential outliers. The air-tear interface is then projected onto a 2D plane and scaled by taking the log of the squared amplitude to create the en face map. Because all OCT measurements contain more than one acquired volume, resulting in more than one en face map per measurement, only the last volume is considered for the evaluation. This corresponds to approximately 4 to 5 seconds after the blink and represents the most stable form of the tear film with the least postblink drifting.^{17,31}

The time to switch between the 2 devices—OCT and LipiView II—and to acquire the corresponding measurements was less than 60 seconds. During all acquisition protocols, subjects were instructed to fixate an internal fixation target and reminded to blink naturally and not excessively. Over all studies, the room temperature was between 20–23°C and the humidity between 40–60%, with nearly constant values over one study day.

The data set used for the presented analysis was retrospectively assembled from baseline measurements before any intervention and control groups of different studies. These studies were designed to investigate the differences in tear film thickness between healthy subjects and dry eye patients or to study the effect and ocular residence time of eye drops and topical lubricants. Owing to the different nature of the studies, the amount of data per subject differs. An overview of the available data is presented (see Supplemental Table 1, Supplemental Digital Content 1, <http://links.lww.com/ICO/B456>).

Definition of Parameters

TFLP Pattern Class

Three classes are defined for the OCT en face maps based on distinct visual characteristics of the TFLP patterns (Fig. 1). The classification was performed according to the following criteria: class 1 is defined as homogeneous (HOM), where the lipid pattern appears generally without holes and without strong local contrast changes. An overall drop in signal intensity toward the edge of the image is still conform because the signal-to-noise ratio drops due to the curvature of the cornea the further the incident laser beam impinges from the corneal apex. Class 2 presents a wavy (WAV) pattern in the largest part of the image. Class 3 is defined as a dotted (DOT) pattern on a dark background. The dots are small points within the image that reveal a high intensity, i.e. reflectivity, that appear in large numbers and close to each other. For ease of reference, we will be referring to class 1, class 2, and class 3, respectively, as HOM, WAV, and DOT for the remainder of the article. The classification was performed by 2 operators (H.S. and R.M.W.) experienced in biomedical imaging and the evaluation of the precorneal tear film and its lipid layer based on OCT technology.

Because one of the study data sets contained measurements with a larger field of view, the en face maps were cropped to represent the same spatial area as the measure-

ments in the other studies, to assure that the classification of the patterns would be comparable.

Lipid Layer Thickness

LLT was measured using the LipiView II Ocular Surface Interferometer (Johnson & Johnson Vision Care, FL). The thickness values are determined using white light interferometry, where the dominant color of the reflected interference pattern is used to estimate a corresponding LLT.^{32,33} The measurement area is in the lower third of the cornea just below the pupil. The estimated values are averaged over 5 seconds of measurement time.

FBUT

FBUT, as an indicator for tear film stability, was measured following the guidelines published in the Report of the International Dry Eye WorkShop 2007³⁴ and is considered a representative value for the TBUT. In brief, 5 µL sodium fluorescein drops (Minims-Fluorescein Sodium 2.0%; Chauvin Pharmaceuticals Ltd, Surrey, United Kingdom) were applied into the conjunctival sac of the eye. The subjects were asked to blink naturally without squeezing to distribute the fluorescein evenly. Within 10 to 30 seconds after fluorescein instillation, the subject was instructed to keep its eyes open without blinking until told otherwise. The time between the last complete blink and first appearance of a dry spot on the tear film was measured. Once a breakup of the tear film was observed, the subject was instructed to blink naturally again.

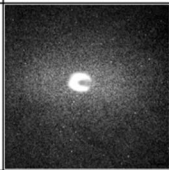
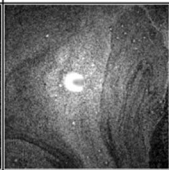
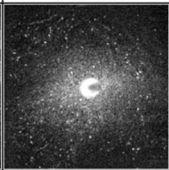
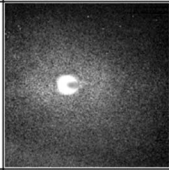
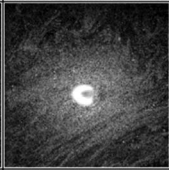
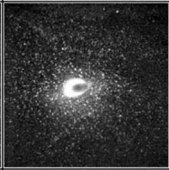
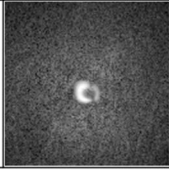
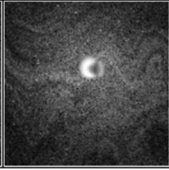
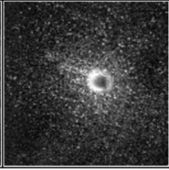
Class	1	2	3
Description	homogeneous	wavy	dotted
Label	HOM	WAV	DOT
Example 1 (2x2 mm ²)			
Example 2 (2x2 mm ²)			
Example 3 (2x2 mm ² , cropped)			

FIGURE 1. Definition and examples of TFLP pattern classes. Central bright spots represent imaging artifacts because of a perpendicular incidence angle of the probe beam. Images depicted in the last line that were acquired with a larger measurement area of 4 × 4 mm² have been cropped to 2 × 2 mm² to show the same region of interest for better comparison.

TABLE 2. Mean Values and SD of LLT, FBUT, and Schirmer Over All Measurements and Within Each of the Defined TFLL Classes

TFLL Pattern Class	LLT	FBUT	Schirmer I Test
Overall	66.3 ± 13.1 nm M = 278	10.7 ± 4.7 s M = 114	21.9 ± 10.3 mm M = 114
HOM	61.3 ± 11.2 nm M = 87	10.4 ± 4.2 s M = 31	23.9 ± 10.0 mm M = 31
WAV	64.7 ± 10.7 nm M = 98	9.3 ± 3.5 s M = 40	23.1 ± 9.4 mm M = 40
DOT	72.7 ± 14.6 nm M = 93	12.2 ± 5.5 s M = 43	19.3 ± 10.9 mm M = 43

M is the number of measurements the values are based on.

Schirmer I Test

The Schirmer I test was performed following the guidelines published in the Report of the International Dry Eye WorkShop 2007.³⁴ A Schirmer paper strip was inserted midway between the middle and outer third of the lower conjunctival sac of the unanaesthetized eye. The subject was then asked to close the eye. The paper strip was removed after 5 minutes, and the Schirmer I test parameter represents the wetted distance of the Schirmer paper after this period.

Statistical Analysis

Statistical analysis was performed using SPSS (IBM SPSS Statistics version 28.0, NY). Mean values and SDs were computed. To investigate the differences in clinical parameters between the different TFLL classes, three linear mixed model analyses were performed. The dependent variables were LLT, FBUT, and Schirmer I test results, respectively. In all models, the TFLL class was used as fixed effect, subject number as random effect, and the eye within a subject as nested random effect. The latter was performed to compensate for repeated measurements of the same eye and of 2 different eyes within the same subject. Estimates β are reported with their 95% confidence intervals, and a P value <0.05 was considered significant.

The intrasubject variability of the TFLL class during time series measurements over 1 hour at a 10-minute interval was assessed using the index of qualitative variation (IQV) as metric. It is defined as

$$IQV = \frac{K}{K-1} \left(1 - \sum_{i=1}^K p_i^2 \right)$$

where K is the number of categories and p_i is the proportion of observations of the i -th category over all time points. For the comparison of 2 different operators, the intraclass correlation coefficient (ICC) and its 95% confidence interval were calculated based on a single rater, absolute agreement, 2-way random-effects model.³⁵

In the following analysis, we assume that the acquisition of the LipiView II and UHR-OCT measurements is

sufficiently close in time to be considered dependent. This hypothesis is founded on reports stating that the TFLL only undergoes minor changes during a blink^{6,9,36} and assumes that the time between the 2 measurements was short enough to prevent a significant amount of blinks.

RESULTS

Mean Values and SDs (Subsets A, B, C, and D)

Mean values and SDs were computed for LLT, FBUT, and Schirmer I test over all measurements and within each TFLL class. The results are presented in Table 2. The mean LLT values were 61.3 ± 11.2 nm, 64.7 ± 10.7 nm, and 72.7 ± 14.6 nm for HOM, WAV, and DOT, respectively.

Difference in LLT Between TFLL Pattern Classes (Subsets A, B, and D)

To investigate the LLT difference between the different lipid map classes, a mixed model analysis was used. The results of this analysis are presented in Table 3. Significant estimates were found for the comparisons HOM versus DOT ($P < 0.001$) and WAV versus DOT ($P = 0.002$).

Difference in FBUT and Schirmer I Test Between TFLL Pattern Classes (Subsets A, B, C, and D)

Two additional mixed model analyses were performed to test for differences between the TFLL classes with respect to FBUT and Schirmer I test values. The results are shown in Table 4 and Table 5 for FBUT and Schirmer I test, respectively. For FBUT, a significant difference was found between WAV and DOT ($P < 0.001$). For Schirmer values, there is no significant difference between any of the classes.

Intrasubject Variability of TFLL Pattern Class Over 1 Hour (Subsets A and B)

The analysis of 7 repeated measurements over 1 hour at a 10-minute interval revealed a mean IQV of $60.0\% \pm 29.9\%$ over 34 eyes of 24 subjects. Four subjects had each 1 eye with

TABLE 3. Pairwise Comparison of Estimates and P Values for the Linear Mixed Model Analysis With LLT as Dependent Variable, TFLL Pattern Class as Fixed Effect, Subject Number as Random Effect, and the Eye Within a Subject as Nested Random Effect

Compared TFLL Pattern Classes	Estimate (nm)	P	95% CI
HOM versus WAV	-2.376	0.070	-4.948 to 0.195
HOM versus DOT	-6.415*	<0.001	-9.244 to -3.586
WAV versus DOT	-4.039*	0.002	-6.623 to -1.454

*Significant at the 0.05 level.

TABLE 4. Pairwise Comparison of Estimates and *P* Values for the Linear Mixed Model Analysis With FBUT as Dependent Variable, TFLL Pattern Class as Fixed Effect, Subject Number as Random Effect, and the Eye Within a Subject as Nested Random Effect

Compared TFLL Pattern Classes	Estimate (s)	<i>P</i>	95% CI
HOM versus WAV	1.286	0.156	−0.500 to 3.073
HOM versus DOT	−1.778	0.054	−3.589 to 0.033
WAV versus DOT	−3.065*	<0.001	−4.745 to −1.385

*Significant at the 0.05 level.

an IQV of zero, i.e. which did not change the pattern once over the period. Two of them were HOM and the other 2 DOT. A total of 17 time series measurements presented 2 of the 3 classes, whereas 13 time series measurements presented each of the 3 classes at least once over an hour.

Intrasubject Similarity of TFLL Pattern Class Between Left and Right Eyes (Subsets A, C, and D)

Using subsets A, C, and D, 40 measurement pairs were analyzed where each subject was imaged in both eyes. Only the first measurement was included from longitudinal time series measurements. In 42.5% of the cases, both eyes of a subject had the same TFLL class.

Interrater Reliability

A second experienced rater (R.M.W.) was tasked to evaluate the en face maps by following the definitions of the different classes in Figure 1 to evaluate the reliability of the classification method. The ICC based on a single rater, absolute agreement, 2-way random-effects model was 89.0% [95% CI (86.5, 91.1)]. All significant comparisons from previous statistical analyses remained significant, and values of estimates were similar to the first rater (H.S.).

DISCUSSION

The correlation between the patterns of OCT TFLL en face maps and clinical parameters of the precorneal tear film was investigated. The evaluated patterns were acquired approximately 4 to 5 seconds after the blink when the tear film was considered most stable. Patterns at earlier time points directly after blinking did not differ in appearance within 1 measurement but were occasionally more prone to motion artifacts that make classification slightly more difficult, and they were thus excluded in this study. The overall means for the parameters LLT, FBUT, and Schirmer are within the expected ranges for healthy subjects reported in the literature.^{37,38}

The mixed model analysis revealed that there is a significant difference in LLT values between TFLL pattern classes. Specifically, a significant difference between DOT

and both HOM and WAV ($\beta_{\text{HOMvsDOT}} = -6.42$ and $\beta_{\text{WAVvsDOT}} = -4.04$) was found, whereas there was no significant difference between the latter two, indicating that DOT represents the thickest type of lipid layer. Considering that the mean LLT in our data set (Table 2) is in the range of 60 to 70 nm, this class is on average approximately 10% thicker than HOM. Although there is no significant difference between HOM and WAV, there seems to be a tendency toward a thicker LLT in WAV than in HOM.

Regarding the FBUT, a statistically significant difference between the TFLL pattern WAV and DOT was detected. Here, considering that the average FBUT is in the range of 10 s in our data set, the estimate of $\beta_{\text{WAVvsDOT}} = -3.065$ would correspond to an approximately 33% shorter TBUT for WAV patterns. Combined with the significantly smaller LLT, this indicates a thinner and less stable TFLL overall for WAV, possibly represented by the wave patterns. King-Smith et al,⁸ using a combined fluorescein and TFLL imaging setup, reported that these darker parts in wave patterns might show an already unstable TFLL over a thinning tear film. In our measurements, which were acquired within the few seconds after blinking, this might lead to an earlier breakup of the tear film when compared with DOT.

The mixed model analysis of the Schirmer I test values revealed no significant difference between any of the 3 classes. Because this test measures a quantity related to the water component of the tear film, i.e. the tear production, it is reasonable to assume that there is no direct correlation with a TFLL pattern class.

In general, it can be noted that the mixed model analyses revealed a significant difference between WAV and DOT for both LLT and FBUT. In comparison with TFLL patterns acquired using other imaging methods than OCT, this result adds a new perspective to the findings in the literature. With Tearscope Plus, i.e. white light interferometry, strong wave patterns are usually indicative of high LLT values,³⁹ whereas spots on a dark background represent lower LLT values when acquired with high-resolution microscopy.²⁰ Slitlamp observations using the pattern classification described by Guillon¹⁶ (Table 1) indicate that wave patterns have intermediate to high noninvasive breakup times.⁴⁰ Owing to the different nature and physical principles of the different imaging methods, it seems that the TFLL patterns acquired with OCT cannot be directly

TABLE 5. Pairwise Comparison of Estimates and *P* Values for the Linear Mixed Model Analysis With Schirmer I Values as Dependent Variable, TFLL Pattern Class as Fixed Effect, Subject Number as Random Effect, and the Eye Within a Subject as Nested Random Effect

Compared TFLL Pattern Classes	Estimate (mm)	<i>P</i>	95% CI
HOM versus WAV	−1.044	0.583	−4.812 to 2.725
HOM versus DOT	2.379	0.240	−1.612 to 6.370
WAV versus DOT	3.423	0.067	−0.247 to 7.092

compared but might give complementary information to the other imaging modalities. Conventional imaging using visible light directly reveals the structural features, while interferometric approaches assess the LLT based on the evaluation of the interference fringes and thickness-dependent reflectance changes. The contrast in the OCT intensity image, on the other hand, is based on the scattering and absorption properties, on the refractive indices of the media and the orientation of the back-reflecting or back-scattering surface with respect to the probe beam. Although the exact origin of the observed TFLL pattern is unclear, it can be assumed that the composition and, more importantly, the arrangement of the molecules that constitute the lipid layer form the basis for its optical appearance. Using molecular dynamics simulations, Wizert and colleagues evaluated the biophysical properties of the TFLL.⁴¹ Based on a system that mimics the lipidome of the tear film, containing water, polar lipids, and nonpolar lipids, different conditions ranging from thermodynamic equilibrium at different surface pressures to nonequilibrium states during a blink were studied. Under strong lateral compression, the monomolecular polar lipid layer that separates the polar lipids from water undulates and further develops irregular bulges. Furthermore, 3-dimensional aggregates of polar lipids occurred in both nonpolar and water subphase of the modeled tear film. The authors suggested that these micelles are formed in course of the highly dynamic conditions during a blink and might act as reservoirs of polar lipids that lead to an increased stability of the tear film. Although the scale of these modeled changes is several orders of magnitude smaller than the resolution of the OCT system used in this study, the molecular phenomena observed here could also be partially responsible for the macroscopic appearance of the TFLL pattern. Here, the undulation and bulging of the polar lipids at the water subphase might lead to varying incidence angles of the OCT probe beam that lead to changes in the back-reflected light intensity and ultimately to a WAV pattern. The highly reflective dots in the DOT patterns might then correspond to the polar lipid aggregations in the nonpolar and particularly the water subphase. The latter assumption is supported by the strongly differing refractive indices—1.48 and 1.34⁴²—for the lipid and the tear film aqueous layer and taking into account that OCT does not directly image the probed sample structure but rather reveals its optical properties. Here, even very small but strong reflectors can lead to a clear intensity signal in the observed TFLL pattern.

One advantage of the analysis of the TFLL pattern is that the involved processing steps are easy to implement and data can be retrieved directly from any OCT anterior segment measurement with resolved tear film without the need for a dedicated acquisition protocol. This also allows for a retrospective analysis of data already recorded, which might provide additional information regarding the precorneal tear film without requiring additional measurements. Given that the precorneal tear film has a thickness in the range of approximately 2 to 8 μm ,^{29,30,43–45} the used OCT system should provide an axial resolution near the lower limit of this range. At poorer resolutions, not only the tear film but also the epithelial front surface fall within the coherence gate of the system, and consequently, only 1 reflection at the corneal front surface

would be revealed. In that case, the resulting reflectance pattern would depend, in addition to the lipid layer thickness (LLT) and the refractive indices of air, lipid, and aqueous layer, also on the thickness of the aqueous layer and the refractive index of the epithelium and might therefore contain information about the epithelial surface. Owing to the smaller difference in refractive indices between aqueous layer and epithelium with values of 1.34 and 1.40,⁴⁶ the intensity signal magnitude and thus the contribution to the qualitative appearance of the reflectance pattern can be assumed to be smaller than that of the lipid pattern. However, an analysis of the reflectance, an effort to determine absolute thickness values,²⁵ would only be possible if the precorneal tear film is resolved in the OCT signal.

Although some of the differences between lipid pattern classes were found to be nonsignificant, a few of them can be seen as indications for underlying relationships, especially when considering the estimates in the larger context of the analysis. The following 2 statements are expressed with caution and require further investigation. First, regarding the LLT, an estimate of $\beta_{\text{HOMvsWAV}} = -2.38$ ($P = 0.07$) reinforces the hypothesis of a thickening LLT in the order of TFLL classes HOM, WAV, and DOT, something that is already apparent from the relative estimates in relation to DOT. Considering the FBUT, an estimate of $\beta_{\text{HOMvsDOT}} = -1.778$ ($P = 0.054$) suggests an increasing FBUT in the order of WAV, HOM, and DOT, which is not the same increasing order of pattern classes when compared with the LLT. There could be 2 different explanations for this: On the one hand, there might be a trade-off between LLT and FBUT in certain lower thickness ranges—here for HOM and WAV—because of some unknown underlying mechanism, potentially regarding the lipid composition. On the other hand, from the technical perspective, the white light interferometry measurements of the LipiView II system determine an average LLT over the whole measurement area. In this case, however, the same amount of lipid molecules might be estimated as a larger LLT when arranged in a wave pattern (crest and troughs) than when arranged as a homogeneous layer. Future investigations are required to explore these hypotheses.

The investigation of repeated measurements at a 10-minute interval over 1 hour revealed that there is a considerable variability among TFLL patterns. In fact, most subjects changed pattern class at least once, and only 4 subjects remained unchanged within this timeframe. Although it is reasonable to assume that the TFLL only undergoes minor changes within a few blinks, it does not seem to be the case for durations in the order of tens of minutes or even hours, where blinking incrementally leads to an overall change in the TFLL pattern. This is consistent with previous reports where both changes in TFLL features after a large number of blinks³⁶ and variations in LLT measured with LipiView II over 1 day were reported.⁴⁷ Furthermore, the TFLL pattern similarity between two eyes of the same subjects is also rather low, given the fact that less than half of the studied subjects had the same pattern in both eyes at the measurement time point. This shows that the TFLL is a very complex structure that can change appearance because of many factors, even in a relatively short timeframe within healthy subjects.

Although this retrospective analysis benefits from the large amount of measurements in the data set, some limitations

should be mentioned. The pattern classification is currently operator dependent and time consuming. Both aspects could be improved by automating the image analysis, either by traditional feature extraction or with convolutional neural networks, of which the latter are perfectly suited for image classification tasks.⁴⁸ Nevertheless, the high ICC shows that the selected pattern classes are easily distinguishable. An additional disadvantage of the current data is that the LLT values and TFLL pattern images are not acquired exactly at the same time. Although it is unlikely that the class of a TFLL pattern switches within a very short timeframe such as it was the case in this data set, this circumstance still impairs the possible precision of the corresponding LLT values. Furthermore, the region of interest on the cornea of both devices, the UHR-OCT and the LipiView II, is not the same. The UHR-OCT measurements were performed over the central corneal region, whereas LipiView II uses the lower part of the cornea for the assessment of the LLT. Here, it would be valuable to have the LLT values directly from the OCT measurement, something that currently remains difficult *in vivo*.²⁵ Further experiments are needed to calibrate the absolute reflectance of the OCT signal within the expected LLT range to overcome this problem.

As a side note, to compare measurements between OCT devices, it is important that the measurement area, lateral sampling density, and the lateral resolution are approximately within the same range. During the evaluation, it was important to crop larger measurement areas to the smallest common denominator because the curvature of the cornea leads to a drop of the SNR at the edges of the image, which can influence the subjective evaluation of the pattern class in some cases. It is also important to acquire the images at a similar time after the blink because the tear film and the TFLL are highly dynamic structures. The acquisition should be a few seconds after the blink so that the TFLL has time to spread after the lid compression, but not too long as to have the appearance of the first breakup regions.

In conclusion, qualitative TFLL patterns that were acquired with OCT are correlated with a significant quantitative difference in LLT and FBUT values. A pattern with dark background and bright spots has on average the thickest TFLL and highest FBUT and might therefore be considered the most stable TFLL. Further investigations could provide additional insights by acquiring the pattern images and LLT within the same measurement and by including patients with DED, potentially revealing new patterns and correlations in nonhealthy subjects.

ACKNOWLEDGMENTS

The authors would like to thank Carl Zeiss Meditec Inc as industrial partner of the Christian Doppler Laboratory for Ocular and Dermal Effects of Thiomers.

REFERENCES

1. Kaido M, Ishida R, Dogru M, Tsubota K. Visual function changes after punctal occlusion with the treatment of short BUT type of dry eye. *Cornea*. 2012;31:1009–1013.
2. Garreis F, Gottschalt M, Schlorf T, et al. Expression and regulation of antimicrobial peptide psoriasin (S100A7) at the ocular surface and in the lacrimal apparatus. *Invest Ophthalmol Vis Sci*. 2011;52:4914–4922.
3. Tiffany JM. The normal tear film. *Dev Ophthalmol*. 2008;41:1–20.
4. Dartt DA. Formation and function of the tear film. In: Levin LA, Nilsson SFE, Hoeve JV, et al, eds. *Adler's Physiology of the Eye*. Edinburgh, London, New York, Oxford, Philadelphia, St. Louis, Sydney, Toronto: Saunders Elsevier; 2011.
5. King-Smith PE, Hinel EA, Nichols JJ. Application of a novel interferometric method to investigate the relation between lipid layer thickness and tear film thinning. *Invest Ophthalmol Vis Sci*. 2010;51:2418–2423.
6. Bron AJ, Tiffany JM, Gouveia SM, et al. Functional aspects of the tear film lipid layer. *Exp Eye Res*. 2004;78:347–360.
7. Millar TJ, Schuett BS. The real reason for having a meibomian lipid layer covering the outer surface of the tear film—a review. *Exp Eye Res*. 2015;137:125–138.
8. King-Smith PE, Reuter KS, Braun RJ, et al. Tear film breakup and structure studied by simultaneous video recording of fluorescence and tear film lipid layer images. *Invest Ophthalmol Vis Sci*. 2013;54:4900–4909.
9. Georgiev GA, Eftimov P, Yokoi N. Structure-function relationship of tear film lipid layer: a contemporary perspective. *Exp Eye Res*. 2017;163:17–28.
10. Butovich IA. Tear film lipids. *Exp Eye Res*. 2013;117:4–27.
11. Butovich IA, Suzuki T. Effects of aging on human meibum. *Invest Ophthalmol Vis Sci*. 2021;62:23.
12. Ong BL, Hodson SA, Wigham T, et al. Evidence for keratin proteins in normal and abnormal human meibomian fluids. *Curr Eye Res*. 1991;10:1113–1119.
13. Willcox MDP, Argueso P, Georgiev GA, et al. TFOS DEWS II tear film report. *Ocul Surf*. 2017;15:366–403.
14. Lemp MA, Crews LA, Bron AJ, et al. Distribution of aqueous-deficient and evaporative dry eye in a clinic-based patient cohort: a retrospective study. *Cornea*. 2012;31:472–478.
15. Stapleton F, Alves M, Bunya VY, et al. TFOS DEWS II epidemiology report. *Ocul Surf*. 2017;15:334–365.
16. Guillon JP. Non-invasive Tearscope Plus routine for contact lens fitting. *Cont Lens Anterior Eye*. 1998;21(suppl 1):S31–S40.
17. Goto E, Tseng SCG. Kinetic analysis of tear interference images in aqueous tear deficiency dry eye before and after punctal occlusion. *Invest Ophthalmol Vis Sci*. 2003;44:1897–1905.
18. Lee JM, Jeon YJ, Kim KY, et al. Ocular surface analysis: a comparison between the LipiView® II and IDRA®. *Eur J Ophthalmol*. 2021;31:2300–2306.
19. Yokoi N, Takehisa Y, Kinoshita S. Correlation of tear lipid layer interference patterns with the diagnosis and severity of dry eye. *Am J Ophthalmol*. 1996;122:818–824.
20. King-Smith PE, Nichols JJ, Braun RJ, Nichols KK. High resolution microscopy of the lipid layer of the tear film. *Ocul Surf*. 2011;9:197–211.
21. Yokoi N, Georgiev GA, Kato H, et al. Classification of fluorescein breakup patterns: a novel method of differential diagnosis for dry eye. *Am J Ophthalmol*. 2017;180:72–85.
22. Kato H, Yokoi N, Watanabe A, et al. Relationship between ocular surface epithelial damage, tear abnormalities, and blink in patients with dry eye. *Cornea*. 2019;38:318–324.
23. Goto E, Tseng SCG. Differentiation of lipid tear deficiency dry eye by kinetic analysis of tear interference images. *Arch Ophthalmol*. 2003;121:173–180.
24. Leitgeb RA. En face optical coherence tomography: a technology review [Invited]. *Biomed Opt Express*. 2019;10:2177–2201.
25. Dos Santos VA, Schmetterer L, Triggs GJ, et al. Super-resolved thickness maps of thin film phantoms and *in vivo* visualization of tear film lipid layer using OCT. *Biomed Opt Express*. 2016;7:2650–2670.
26. Thai LC, Tomlinson A, Doane MG. Effect of contact lens materials on tear physiology. *Optom Vis Sci*. 2004;81:194–204.
27. Remeseiro B, Oliver KM, Tomlinson A, et al. Automatic grading system for human tear films. *Pattern Anal Appl*. 2014;18:677–694.
28. World Medical A. World Medical Association Declaration of Helsinki: ethical principles for medical research involving human subjects. *JAMA*. 2013;310:2191–2194.
29. Werkmeister RM, Alex A, Kaya S, et al. Measurement of tear film thickness using ultrahigh-resolution optical coherence tomography. *Invest Ophthalmol Vis Sci*. 2013;54:5578–5583.
30. Aranha Dos Santos V, Schmetterer L, Groschl M, et al. *In vivo* tear film thickness measurement and tear film dynamics visualization using

- spectral domain optical coherence tomography. *Opt Express*. 2015;23:21043–21063.
31. Yokoi N, Yamada H, Mizukusa Y, et al. Rheology of tear film lipid layer spread in normal and aqueous tear-deficient dry eyes. *Invest Ophthalmol Vis Sci*. 2008;49:5319–5324.
 32. Goto E, Dogru M, Kojima T, Tsubota K. Computer-synthesis of an interference color chart of human tear lipid layer, by a colorimetric approach. *Invest Ophthalmol Vis Sci*. 2003;44:4693–4697.
 33. Markoulli M, Duong TB, Lin M, Papas E. Imaging the tear film: a comparison between the subjective keeler tearscope-plus™ and the objective Oculus® keratograph 5M and LipiView® interferometer. *Curr Eye Res*. 2018;43:155–162.
 34. DEWS. Methodologies to diagnose and monitor dry eye disease: report of the diagnostic methodology subcommittee of the international dry eye Workshop (2007). *Ocul Surf*. 2007;5:108–152.
 35. Koo TK, Li MY. A guideline of selecting and reporting intraclass correlation coefficients for reliability research. *J Chiropr Med*. 2016;15:155–163.
 36. Yokoi N, Bron AJ, Georgiev GA. The precorneal tear film as a fluid shell: the effect of blinking and saccades on tear film distribution and dynamics. *Ocul Surf*. 2014;12:252–266.
 37. Hwang H, Jeon HJ, Yow KC, et al. Image-based quantitative analysis of tear film lipid layer thickness for meibomian gland evaluation. *Biomed Eng Online*. 2017;16:135.
 38. Tian L, Qu JH, Zhang XY, Sun XG. Repeatability and reproducibility of noninvasive keratograph 5M measurements in patients with dry eye disease. *J Ophthalmol*. 2016;2016:8013621.
 39. Remeseiro B, Bolon-Canedo V, Peteiro-Barral D, et al. A methodology for improving tear film lipid layer classification. *IEEE J Biomed Health Inform*. 2014;18:1485–1493.
 40. Maissa C, Guillon M. Tear film dynamics and lipid layer characteristics—effect of age and gender. *Cont Lens Anterior Eye*. 2010;33:176–182.
 41. Wizert A, Iskander DR, Cwiklik L. Organization of lipids in the tear film: a molecular-level view. *PLoS One*. 2014;9:e92461.
 42. Patel S, Tutchenko L. The refractive index of the human cornea: a review. *Cont Lens Anterior Eye*. 2019;42:575–580.
 43. King-Smith PE, Fink BA, Fogt N, et al. The thickness of the human precorneal tear film: evidence from reflection spectra. *Invest Ophthalmol Vis Sci*. 2000;41:3348–3359.
 44. King-Smith PE, Fink BA, Hill RM, et al. The thickness of the tear film. *Curr Eye Res*. 2004;29:357–368.
 45. Schmidl D, Witkowska KJ, Kaya S, et al. The association between subjective and objective parameters for the assessment of dry-eye syndrome. *Invest Ophthalmol Vis Sci*. 2015;56:1467–1472.
 46. Patel S, Marshall J, Fitzke FW III. Refractive index of the human corneal epithelium and stroma. *J Refract Surg*. 1995;11:100–105.
 47. Finis D, Pischel N, Borrelli M, et al. [Factors influencing the measurement of tear film lipid layer thickness with interferometry]. *Klin Monbl Augenheilkd*. 2014;231:603–610.
 48. Pfister M, Stegmann H, Schutzenberger K, et al. Deep learning differentiates between healthy and diabetic mouse ears from optical coherence tomography angiography images. *Ann N Y Acad Sci*. 2021;1497:15–26.